Supporting Information for:

"Isotope-Edited FTIR of Alkaline Phosphatase Resolves Paradoxical Ligand Binding Properties and Suggests a Role for Ground State Destabilization"

Logan D. Andrews[a], Hua Deng[b], and Daniel Herschlag[a,c,d]

[a]Department of Chemical and Systems Biology and [c]Department of Biochemistry, Stanford University, Stanford, California 94305. [b]Department of Biochemistry, Albert Einstein College of Medicine, 1300 Morris Park Avenue, Bronx, New York 10461

[d]Corresponding author:

Dept. of Biochemistry, B400

Stanford University

Stanford, CA 94305-5307

650-723-9442 (telephone)

650-723-6783 (fax)

herschla@stanford.edu

AP Catalytic Rate Enhancement and Affinity for the Substrate Transition State

The rate enhancement provided by AP is the ratio of the catalyzed and uncatalyzed phosphate monoester hydrolysis rate constants – the enzyme reacts with the phosphate monoester dianion so for comparison the uncatalyzed rate constant considered must also be for the dianion. Previous measurements of the uncatalyzed phosphate monoester dianion hydrolysis reaction estimated that the first order rate constant is 2×10^{-20} s^{-1} for attack by water at 25 ºC.[1] Dividing the first-order rate constant by the concentration of water (55 M) yields a second order rate constant of 3.6×10^{-22} $M^{-1}s^{-1}$. AP catalyzes this hydrolysis with a second-order rate constant (k_{cat}/K_M) of 1.2×10^{6} $M^{-1}s^{-1}$, giving a ration that represents the rate enhancement of 3×10^{27}-fold.[2]

Reaction rate constants can be converted to apparent equilibrium constants using Eyring's transition state theory by eq S1 and S2

$$k_{uncat} = (kT/h)K^{\ddagger}_{uncat} \quad (S1)$$

$$k_{enzyme} = (kT/h)K^{\ddagger}_{enzyme} \quad (S2)$$

where k is the Boltzmann constant, T is the absolute temperature, and h is Planck's constant. The equilibrium constants are defined in Figure S1. These equilibrium constants can be expressed as free energy changes by the standard relationship between free energies and equilibrium constants (eq S3 and S4; R is the gas constant; assuming a standard state of 1M).

$$\Delta G^{\ddagger}_{uncat} = - RT\ln(K^{\ddagger}_{uncat}) \quad (S3)$$

$$\Delta G^{\ddagger}_{enzyme} = - RT\ln(K^{\ddagger}_{enzyme}) \quad (S4)$$

The difference between the free energies from eq S3 and S4 gives the energetic stabilization of the reaction transition state by the enzyme. This energetic difference can be expressed as,

$$\Delta\Delta G^{\ddagger} = RT\ln(k_{enzyme}/k_{uncat}) \quad (S5)$$

which for a rate enhancement of 10^{27}-fold at room temperature (298 K) corresponds to 37 kcal/mol. This energetic difference is also equivalent to the enzyme's theoretical affinity for the substrate transition state ($S^{‡}$), which is described by the equilibrium constant K_T in Figure S1. The following relationships illustrate this equivalence:

$$K^{‡}_{enzyme} = K^{‡}_{uncat} \times K_T \quad \text{(S6)}$$

$$K^{‡}_{enzyme}/K^{‡}_{uncat} = K_T \quad \text{(S7)}$$

$$K_T = k_{enzyme}/k_{uncat} = e^{\Delta\Delta G^{\dagger}/RT} \quad \text{(S8)}$$

Thus, the theoretical affinity of AP for the phosphate monoester dianion transition state is also 37 kcal/mol. The theoretical affinity reflects the binding of the enzyme to the transition state while accompanied by the replacement of water by the active site Ser102 for the enzyme-catalyzed reaction. The energetics of these two processes cannot be separated but correspond to an overall energetic change of 37 kcal/mol upon formation of the enzyme transition state complex.

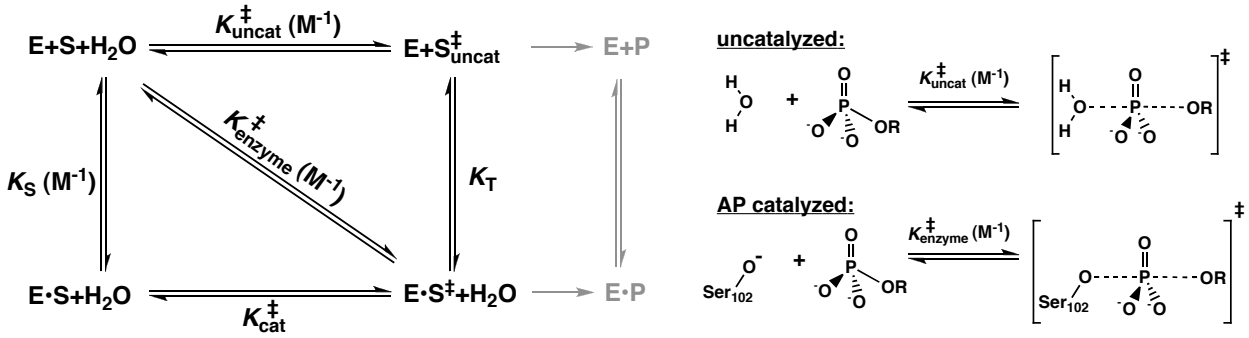

Figure S1. General reaction scheme for an enzymatic reaction and the corresponding bimolecular nonenzymatic reaction. From transition state theory, equilibrium constants between ground states and transition states can be related to observed rate constants as described in text. As thermodynamics is pathway independent the ratio of $K^{‡}_{enzyme}$ and $K^{‡}_{uncat}$ is equal to K_T, the formal equilibrium constant for transition state binding to the enzyme.

Evidence from Prior Studies That the P_i Dianion Does Not Release a Proton to Solution Upon Binding AP

Free inorganic phosphate (P_i) can exist in several different ionic forms depending on the solution pH (Scheme S1; pK_a's reported for 25 °C, 0.5 M ionic strength[3]), and therefore AP could, in principle, bind any or multiple P_i species from solution.

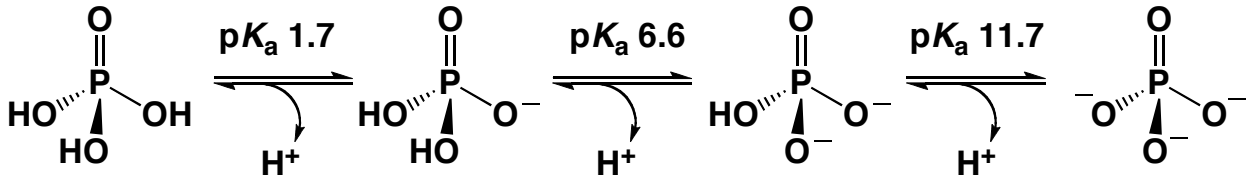

Scheme S1

The binding affinity of AP for P_i measured across pH reveals the number of protons taken up by the complex or released to solution upon association of the preferred solution P_i species and predominate free AP species at each pH. Previous binding studies show a log linear increase in AP•P_i affinity as the pH is raised from 4.5 to ~6 (Figure S2A).[4] Over this pH range the P_i dianion (HPO_4^{2-}) becomes more and more populated in solution as the P_i monoanion ($H_2PO_4^{1-}$) pK_a is ~6.6 under these conditions. The log-linear increase in AP binding affinity with a slope of 1 at low pH then suggests that AP has no measurable affinity for $H_2PO_4^{1-}$ or equivalently, that a proton is lost upon binding. The slope of 1 levels to zero with an apparent pK_a of 6.6, indicating no gain or loss of a proton upon binding and consistent with binding of HPO_4^{2-} in the region above 6.6. This model, with HPO_4^{2-} binding, is represented in eq S9 and is the simplest model consistent with the data. (So far we consider only the data up to pH 8.)

$$AP + HPO_4^{2-} \rightleftharpoons AP \bullet (H^+)PO_4^{3-} \qquad \text{(S9)}$$

We next consider an alternative model for P_i binding in which HPO_4^{2-} binds but loses its proton to solution, as illustrated in eq S10. This is the model that we note in the main text is ruled out by prior data.

$$AP + HPO_4^{2-} \rightleftharpoons AP \bullet PO_4^{3-} + H^+ \quad \text{(S10)}$$

In the eq S10 model, the binding of HPO_4^{2-} occurs with loss of a proton and is thus thermodynamically equivalent to the binding of the free P_i trianion (PO_4^{3-}) from solution. The observed P_i binding affinity would therefore reflect the available population of PO_4^{3-} at any given pH. At pH values below 6.6, *two* protons must be lost to give PO_4^{3-}, so that a drop in binding affinity with a slope of 2 (log-linear) is predicted. The experimentally observed slope of 1 at the acidic pH values therefore, provides evidence against this model.

Further, the binding of P_i levels off at pH values above 6.6, the pK_a for formation of HPO_4^{2-}. If PO_4^{3-} bound from solution then an additional proton would need to be lost and binding would continue to increase log-linearly with a slope of 1 above pH 6.6, which is not observed.

Additional support for the model of eq S9 comes from the observation that the observed pK_a in pH-dependences such as that in Figure S2A give different pK_a's for different ligands (or substrates), with the pK_a mirroring the solution pK_a of the binding or reacting group[4] – i.e. the observed pK_a reflects the known pK_a of the ligand. Nevertheless, complexities from protonation and deprotonation events on the enzyme are possible. The simplest data that rule out such complexities (for data below pH 8) are shown in Figure S2B for binding of tungstate to AP and are described below.

To isolate any potential protonation events associated with AP and not the binding ligand, the pH-dependent binding affinity of a molecule that does not have a pK_a in the pH region of interest was measured.[4] The AP binding affinity for tungstate, which has a single pK_a of ~4, was

measured as a function of pH (Figure S2B). The binding is flat from pH 4.5 to 8, indicating that there are no enzymatic protonation or deprotonation events that affect ligand binding across this pH range, and the model of eq S9 is strongly supported whereas that of S10 is ruled out.

The pH-dependence for tungstate binding does reveal a complexity above pH 8, but this complexity also leads to support for the eq S9 model and evidence against the eq S10 model – i.e. formal binding of HPO_4^{2-} and not PO_4^{3-}. The pH dependence for tungstate binding reveals a log-linear decrease in binding affinity at pH values above 8 with a slope of one, as observed for P_i binding (Figure S2A and S2B). Because the observed decrease cannot be associated with a pK_a of free tungstate, this decrease must represent a deprotonation event associated with AP itself, with an inactivating pK_a of 8. [The pK_a is observed in pH dependencies of binding, as in Figure S2, and catalytic activity (see ref. 4; data not shown).] The model for tungstate binding that follows from the above results is described by eq S11.

$$\begin{array}{ccc} AP_H + WO_4^{2-} & \rightleftharpoons & AP_H \bullet WO_4^{2-} \\ \Updownarrow & & \\ AP_{inactive} + WO_4^{2-} + H^+ & & \end{array} \qquad \text{(S11)}$$

Given this inactivating pK_a of 8, if HPO_4^{2-} binds then binding should weaken log-linearly above pH 8, as there are no pK_a's for P_i from 6.6 to >11 (Scheme S1). This dependence is observed in Figure S2A. In contrast, if PO_4^{3-} were to bind, it would have to lose a proton while AP would need to gain a proton to be in a binding-active state, so that a flat pH-dependence for binding would be predicted. The observed log-linear dependence with slope -1 then provides additional evidence ruling out model of eq S10. In summary, both the pH-dependent P_i and tungstate data support the model of eq S9 and rule out that of eq S10. While eq S9 requires that the HPO_4^{2-} proton remain part of the bound complex, the pH-dependent data do not reveal where

the proton is within the complex – i.e. if the proton remains on P_i or gets transferred to AP. An FTIR approach was used to distinguish between these possibilities as described in the main text.

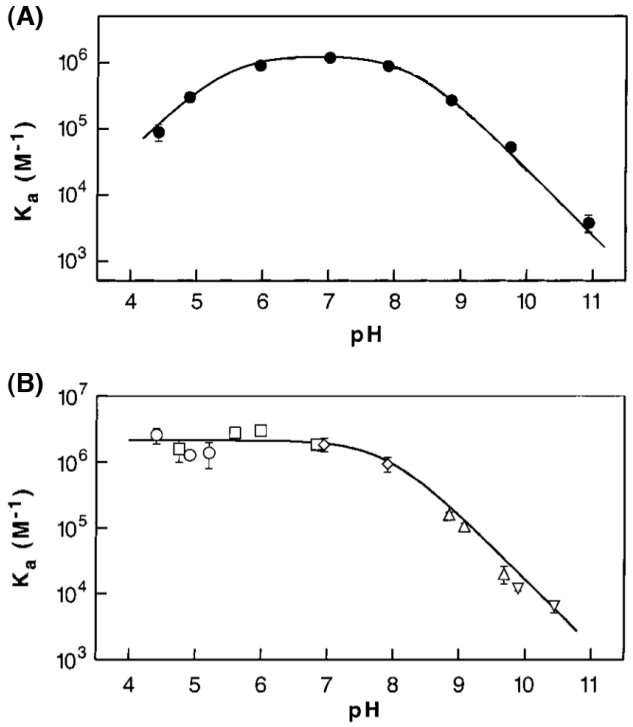

Figure S2. The pH dependence of AP for phosphate (A) and tungstate (B) binding. Data are from ref. 4 and affinity values were determined by inhibition of 2-fluoroethyl phosphate hydrolysis (pH 4.5-9.0) and inhibition of *p*NPP hydrolysis (pH 8-11) with [S] << K_M, such that K_i is expected to be the K_d. The observed inhibition constants, which were converted to K_a's for the plots above, were the same for both substrates at a given pH. For phosphate binding (A), the measurements at low pH are corrected for the amount of covalently bound P_i. Nonlinear-least-squares fit of the data to a model for two ionizations ($K_a^{Pi\ obs} = (K_a^{Pi\ max})/(1 + [H^+]/K_1 + K_2/[H^+])$) gave p$K_a$ values of 5.5 +/- 0.2 and 8.2 +/- 0.2. The acidic pK_a does not correspond exactly to the expected $H_2PO_4^{1-}$ pK_a because further analysis of the pH-dependence not described here suggests an enzymatic group with a pK_a of ~5.5 provides ~5-fold stimulation when protonated (see ref. 4). This enzymatic stimulation offsets the expected acidic limb of P_i binding by about 1 pK_a unit (pK_a $H_2PO_4^{1-}$ ~6.6). For tungstate binding (B) the different symbols represent different buffers used and the line represents the best fit of a model for a single ionization at pK_a = 8.0 +/- 0.2. There is no acidic limb because the tungstate pK_a is <4.5. (Figure adapted from ref. 4)

Evidence from Prior Studies that the AP Active Site Nucleophile, Ser102, has a p$K_a \leq 5.5$

The pH-dependent P_i binding studies discussed in the previous section show two limbs, one acidic and one basic, that are log-linear each with a slope of one. The pK_a associated with the

acidic limb corresponds to the expected pK_a of the P_i ligand and for ligands without such a pK_a there is no pH dependence down to pH 4.5.[4] The pK_a of the basic limb of any AP pH profile is independent of the ligand pK_a or even the presence of a titratable group on the ligand, indicating that this limb of the profile is associated with a deprotonation event on the enzyme, as discussed above and in ref. 4.

It is possible, in principle, that this deprotonation event at basic pH could be associated with a titration of the AP active site nucleophile, Ser102. This model requires that SerOH (and not $SerO^-$) be the active form of the nucleophile and that its pK_a be 8. This requirement holds despite the greater reactivity of alkoxides than their corresponding alcohols, rendering this model unlikely, although the small values of β_{NUC} for reactions of phosphate monoesters suggest that the actual difference in reactivity may be modest (for review see ref. 2). In addition, the pK_a of water, which has a similar pK_a as alcohols such as serine, is lowered from 16 to 8-10 when coordinated by Zn^{2+} (Scheme S2);[5] the presence of a Zn^{2+}-bimetallo site, and possibly the nearby Mg^{2+} ion in the AP active site (see Scheme 1B main text), would be expected to lower the pK_a of Ser102 considerably below the range of 8-10. Indeed, pH-dependencies for other Zn^{2+} bimetallo enzymes are consistent with SerOH pK_a values <6,[6,7] and carbonic anhydrase with only a single Zn^{2+} ion has a pK_a of 6.7 for its Zn^{2+}-coordinated water.[8] Given the above, it is highly unlikely that the pK_a of 8 that leads to decreased binding and reactivity corresponds to formation of Ser102 alkoxide in AP, with this anion being unable to participate in the enzymatic reaction. As there is no other enzymatic pK_a from 5.5-11, it is likely that the pK_a of Ser102 of AP is $\leq$ 5.5.

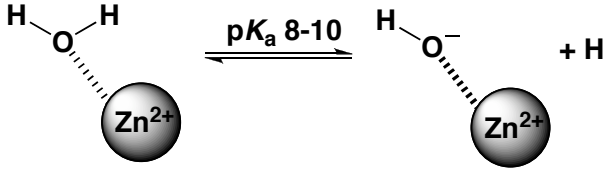

Scheme S2

The following provides additional evidence for the presence of Ser102 alkoxide across the observed pH profile. To assess whether such a protonation event at Ser102 was responsible for the basic limb of the P_i binding affinity profile, previous authors considered the pH-dependent equilibrium between the covalent phosphoserine intermediate and noncovalently bound P_i.[4] Previous pH-dependent P_i binding results suggest that HPO_4^{2-} is the species formally bound by the enzyme (see section above). It has also been established by ^{31}P-NMR[9-11] and ^{32}[P_i]-labeling studies[12] that AP forms a covalent bond at Ser102 with P_i at low pH (see main text). Two possible equilibria are shown in eq S12 and S13 depicting the formation of the covalent adduct starting with either protonated or deprotonated Ser102.

$$AP^{SerOH} + HPO_4^{2-} \rightleftharpoons AP^{SerOH} \bullet (H)PO_4^{3-} \rightleftharpoons AP^{SerO\text{-}PO_3^{2-}} + H_2O \qquad \text{(S12)}$$

$$AP^{SerO^-} + HPO_4^{2-} \rightleftharpoons AP^{SerO^-} \bullet (H)PO_4^{3-} \rightleftharpoons AP^{SerO\text{-}PO_3^{2-}} + {}^-OH \qquad \text{(S13)}$$

Eq S12 predicts that the formation of the covalent AP-P_i species would be pH-independent as no net transfer of protons is involved in the equilibrium. In contrast, eq S13 predicts a pH-dependence as $^-$OH is released upon formation of the covalent species. The formation of the AP-P_i covalent species at low pH is pH-dependent, consistent with the equilibrium depicted in eq S13 but not of that depicted in eq S12.[4] This experimental observation provides further evidence against SerOH, with a pK_a of 8, acting as the active nucleophile.

In summary, the observations and arguments above suggest that neither the acidic nor basic limb observed in the AP•P_i binding affinity pH profile is associated with a titration of Ser102. The acidic limb is accounted for by the ligand pK_a, and the basic limb is not consistent with a Ser102 titration as suggested by known pK_a perturbations from Zn^{2+} and by the covalent adduct formation analysis above. Additional evidence against a Ser102 pK_a corresponding to the basic limb is also discussed further in ref. 4. As the data in the AP•P_i pH binding profile goes

down to pH 4.5 an upper limit for the Ser102 pK_a could be set by this pH. However, the pH profile is complicated by a stimulatory pK_a at ~5.5,[4] so we estimate a conservative assignment of the Ser102 pK_a corresponding to the upper limit set by this pK_a of 5.5.

Interpretation of Potential FTIR Signals of AP-phosphoserine at pH 5.0

As described in the main text, previous ^{31}P-NMR and biochemical binding studies have indicated that approximately half of AP-bound P_i at pH 5.0 is bound covalently to Ser102. Thus, it was expected that the FTIR spectrum of AP-bound P_i at pH 5.0 would reflect equal vibrational contributions from the noncovalently bound P_i species and the covalently bound phosphoserine monoester.

The first expectation that the pH 5.0 FTIR spectrum should contain peaks associated with noncovalently bound P_i, was convincingly observed (Figure S3, red arrows). A prominent peak in the pH 5.0 spectrum at 1015 cm^{-1} has the same frequency and general shape as the peak observed in the pH 8.0 FTIR spectrum, which contains only contributions from noncovalently bound P_i. In addition, this peak corresponds to the prominent peak observed in the standard PO_4^{3-} solution spectrum, suggesting that the noncovalently bound P_i species in both the pH 8.0 and pH 5.0 samples is PO_4^{3-} as discussed in the main text. The corresponding ^{18}O-PO_4^{3-} negative peak that was expected at 972 cm^{-1} based on the pH 8.0 AP and standard solution PO_4^{3-} spectra was not as clearly observed in the pH 5.0 spectrum. In the pH 5.0 spectrum this peak is likely masked by the noise that appears at wavenumbers below 975 cm^{-1} by uncertainties in obtaining a reliable subtracted background. However, there is evidence of a negative peak below 1000 cm^{-1}, as expected, but this peak appears to be only partially observed due to the background issues.

Additional peaks appear in the pH 5.0 spectrum above 1050 cm^{-1}. A relatively small positive peak is observed at 1072 cm^{-1} (Figure S3, green arrow). This peak likely arises from a small population of unbound $H_2PO_4^{1-}$ in the sample because the frequency of the peak most closely corresponds to the positive peak observed at 1077 cm^{-1} in the standard P_i^{1-} solution spectrum. The corresponding negative peak for this species in the pH 5.0 AP spectrum (expected around 1038 cm^{-1}) is masked by the more intense 1015 cm^{-1} peak.

The other peaks observed in the pH 5.0 spectrum are more difficult to interpret because the frequencies of these peaks do not correspond to any of the P_i solution spectra. Based on the second expectation at pH 5.0, that approximately half of the P_i is bound covalently, we suggest that these peaks may correspond to the vibrational properties of the phosphoserine monoester. For alkyl phosphate monoester model compounds, observed IR frequencies fall within the 1089-1110 cm^{-1} range (for the asymmetric stretching frequency).[13] In our pH 5.0 spectrum there is a pair of prominent peaks within this range (negative peak, 1089 cm^{-1}; positive peak, 1107 cm^{-1}; black arrows in Figure S3). This peak pair presumably arises from the phosphoserine covalent species.

Interestingly, the wavenumber difference between this peak pair is smaller (18 cm^{-1}) than expected for a $^{16}O/^{18}O$-labeled phosphate group based on the wavenumber differences observed for peak pair frequencies of P_i and other phosphate monoesters (25-45 cm^{-1} shifts typically observed for these compounds upon ^{18}O-labeling). One explanation for the unusual peak pair difference observed is that the vibrational properties of the AP phosphoserine are perturbed by influences from the active site relative to the expected vibrational properties from a solution version of the phosphoserine monoester. This explanation is consistent with previous interpretations of the AP phosphoserine ^{31}P-NMR chemical shift; the chemical shift of the AP

phosphoserine species is shifted downfield by ~6 ppm from the expected chemical shift of the small molecule phosphoserine.[9] This proposed perturbation may also influence the vibrational properties of covalently bound phosphate resulting in the unexpected peak pair frequency differences observed in our pH 5.0 FTIR spectrum. Also, changes in the Zn^{2+}-P_i interactions in the covalent complex relative to the noncovalent complex could result in vibrational mode decoupling since only one or two of the P-O bonds in P_i interact with the Zn^{2+} ions. Such a change in interaction energy could break the vibrational symmetry of the bound P_i molecule resulting in peak splitting or pattern changes to the AP-bound phosphoserine spectrum. These and other possiblities make it difficult to directly assign peaks to the phosphoserine AP covalent species. But in the absence of further tests, we adopt the most likely explanation that the 1089 and 1107 cm^{-1} peaks correspond to the covalently bound P_i species expected at pH 5.0.

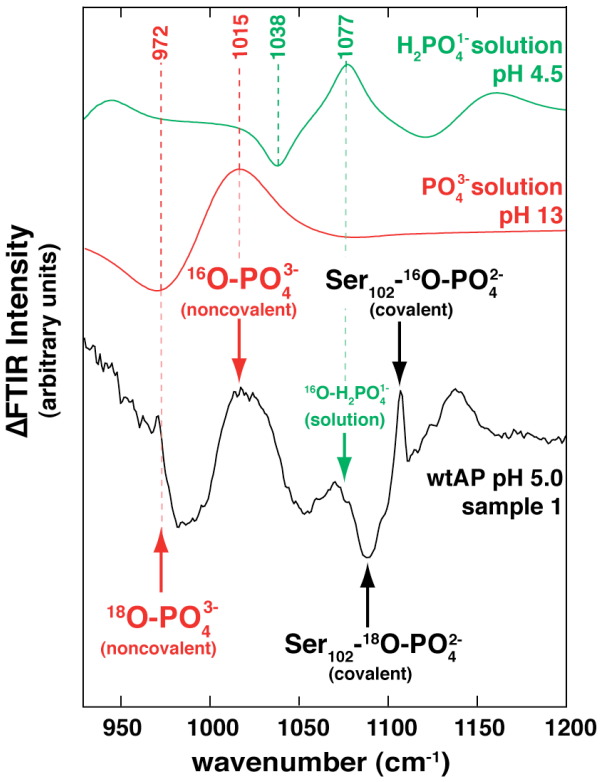

Figure S3. [^{18}O]-P_i edited FTIR difference spectra of P_i in solution and AP-bound at pH 5.0. FTIR difference spectrum between ^{16}O-P_i and ^{18}O-P_i at pH 4.5 (green) or pH 13 (red). FTIR

difference spectrum between AP•^{16}O-P_i and AP•^{18}O-P_i (4.6 mM AP, 2.8 mM P_i) in 10 mM NaAcetate, pH 5.0, 100 mM NaCl, 100 μM $ZnCl_2$, and 1 mM $MgCl_2$ (Sample 1, black). Red arrows mark the expected peak frequencies for noncovalently bound PO_4^{3-} corresponding to the PO_4^{3-} solution spectrum. The green arrow indicates the expected positive peak frequency for $H_2PO_4^{1-}$ from the standard $H_2PO_4^{1-}$ solution spectrum above. This relatively small peak likely arises from an unbound population of $H_2PO_4^{1-}$. The black arrows indicate the positive and negative peaks proposed to arise from the AP phosphoserine covalent species. The unmarked positive peak at 1138 cm^{-1} is unidentified and may also arise from a relatively small contribution of unbound $H_2PO_4^{1-}$ although the correspondence to the $H_2PO_4^{1-}$ solution spectrum is less than expected.

Analysis for Potential Coincidental Shifts of Observed FTIR Spectra

The observed AP with P_i FTIR pH 8.0 difference spectrum could coincidentally reflect HPO_4^{2-} with shifted vibrational properties if the peak pair observed at 1015 and 972 cm^{-1} actually correspond to the peak pair associated with the asymmetric stretching frequencies at 1081 and 1044 cm^{-1} of the solution HPO_4^{2-} (Figure S4). For the observed peak pair to correspond to the HPO_4^{2-} asymmetric peak pair, a shift of -66 cm^{-1} upon binding would be required (Figure S4A). A shift this large to the solution vibrational frequencies of the P_i ligand upon protein binding would be unprecedented[14-16]. Furthermore, we do not expect the observed peak pair to correspond to the asymmetric solution HPO_4^{2-} peaks based on the difference between the frequencies of the positive and negative peak pair. The frequency difference between the positive and negative peaks of the HPO_4^{2-} solution spectrum is 37 cm^{-1} while the difference between the observed peaks is 43 cm^{-1}. Therefore, the difference between the positive and negative peaks of the observed spectrum does not agree with the peak difference of the asymmetric vibrational frequencies of the solution HPO_4^{2-}. This difference further suggests that the observed AP with P_i spectrum does not represent the asymmetric stretching frequencies for HPO_4^{2-}.

We also considered the opposite coincidental frequency shift that would result in the observed peaks corresponding to the symmetric stretching frequencies of the solution HPO_4^{2-} (Figure 4B). If the symmetric peak frequencies of the HPO_4^{2-} ligand at 947 and 990 cm^{-1} shifted by +25 cm^{-1} upon binding, then the observed peaks in the AP sample would correspond to the symmetric stretching frequencies of bound HPO_4^{2-}. This frequency shift would not be unprecedented; however, given the observation window of the measurement, we would then also expect to observe the correspondingly shifted asymmetric peaks of the HPO_4^{2-} at 1106 and 1069 cm^{-1}, assuming that the protein induced frequency shifts effect both symmetric and asymmetric stretching frequencies equally. We do not observe an additional set of peaks in this frequency range, again suggesting that the observed spectrum does not reflect HPO_4^{2-} with shifted vibrational properties.

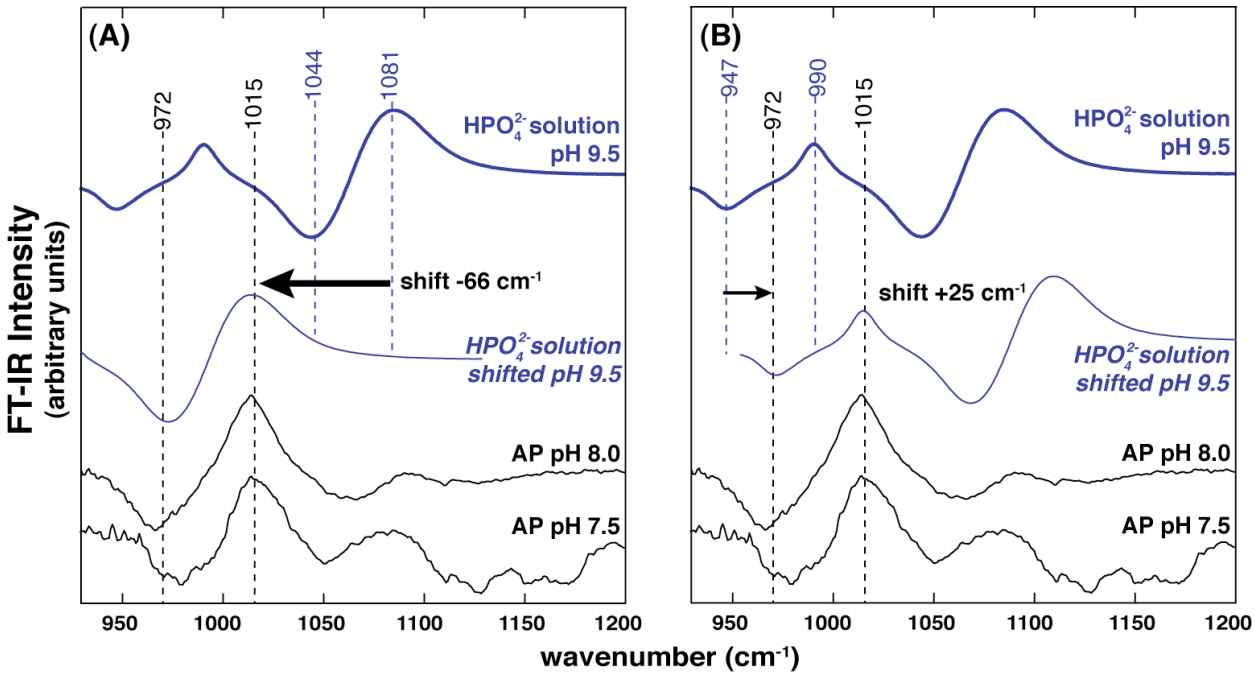

Figure S4. A comparison of the HPO_4^{2-} solution spectrum and the hypothetical shifts of this spectrum that would be required to resemble the observed P_i-bound AP spectra. (A) If the peaks at 1015 and 972 cm^{-1} in the observed spectra reflect the HPO_4^{2-} asymmetric peak pair, an unprecedented shift to the solution-like asymmetric vibrational frequency of HPO_4^{2-} of 66 cm^{-1}

would be required upon AP-binding. Note that the difference between the asymmetric peak pair of HPO_4^{2-} (at 1081 and 1044 cm^{-1}) is larger than the difference between the peaks in the observed P_i-bound AP spectra. (B) If the observed peaks in the P_i-bound AP spectra reflect the HPO_4^{2-} symmetric peak pair at 990 and 947 cm^{-1} a shift to the solution-like vibrational frequency of HPO_4^{2-} of 25 cm^{-1} would be required. Note, however, that this shift also leaves the asymmetric peak pair within the observation window. This peak pair is not observed in the P_i-bound AP spectra.

Determination of PO_4^{3-} Affinity for Deprotonated Ser102 AP

The PO_4^{3-} affinity for deprotonated Ser102 AP can be estimated by measuring the P_i affinity across a pH range. In principle, the observed P_i binding at a given pH can reflect the binding contributions of any of the P_i species. The results presented in the main text indicate that the observed P_i affinity in the neutral pH range reflects the binding of HPO_4^{2-} specifically (resulting in an internal proton transfer presumably to Ser102 and the formation of bound PO_4^{3-}). The contribution of HPO_4^{2-} binding to the overall observed P_i binding is expected to be constant at pH values well below the HPO_4^{2-} pK_a (11.7) as the proportion of HPO_4^{2-} in solution remains nearly constant up to pH values approaching the pK_a. However, as the pH approaches the HPO_4^{2-} pK_a and the proportion of PO_4^{3-} in solution increases, the overall observed P_i affinity could start to reflect a binding contribution from PO_4^{3-}. Any influence of PO_4^{3-} on the observed P_i affinity will depend on the solution pH and the PO_4^{3-} affinity relative to the apparent HPO_4^{2-} affinity. An increase in the observed P_i affinity as the pH is raised would indicate a binding contribution from PO_4^{3-}. As all of the Ser102 AP will be deprotonated at these pH values (p$K_a \leq 5.5$), PO_4^{3-} binding that increases as pH increases would be to deprotonated Ser102 AP.

The observed pH-dependent P_i binding to AP is complicated by an inactivating pK_a of ~8.2 associated with free AP.[4] Nevertheless, this inactivating titration can be accounted for and if PO_4^{3-} makes a binding contribution at higher pH values, we still expect to see an upward trend

from the observed affinity. To ensure that AP remains functional even at very high pH values, we plotted the *p*-nitrophenyl phosphate (*p*NPP) hydrolysis activity throughout the pH range. Reactions were measured to completion under conditions in which [S] < K_M as described previously.[4,17] As *p*NPP has no titratable protons in this pH range we expected to observe a continuous log linear decrease in activity reflecting only the pK_a associated with AP. Negative deviations from this trend would have indicated unpredictable loss of enzyme activity (potentially due to unfolding). We observed a simply behaved pH-dependence of *p*NPP activity out to pH 11.4 (Figure S5A) that could be fit to eq S14 for two rate-controlling ionizations (also as reported previously to pH 11, ref. 17). Loss of activity was observed at pH > 11.4 and thus, we only carried out the P_i affinity measurements to this pH.

$$\left(k_{cat}/K_M\right)^{obs} = \frac{\left(k_{cat}/K_M\right)^{max}}{\left(1+10^{pK_a^{acidic}-pH}+10^{pH-pK_a^{basic}}\right)} \quad \text{(S14)}$$

The P_i affinity data from pH 7.0-11.4 is shown in Figure S5B. The P_i affinity data shows no significant deviation from the expected HPO_4^{2-} affinity trend even up to pH 11.4 where the proportion of PO_4^{3-} in solution is above 10%. Because no influence of PO_4^{3-} binding was detected we could only set a lower limit for the dissociation constant of PO_4^{3-} binding to deprotonated Ser102 AP ($K_a^{SerO^- \bullet PO_4^{3-}}$). To estimate the lower limit, eq S15, derived from Scheme S3, was used to fit the data from pH 7.0-11.0. The PO_4^{3-} affinity in eq S15 was fixed at a series of values corresponding to decreasing $K_a^{SerO^- \bullet PO_4^{3-}}$ values as shown in Figure S5B. The observed deviations of the fits to the data at pH 11.0-11.4 (open circles) were used to set a lower limit for the PO_4^{3-} affinity. Clear deviations from the high pH data are observed if $K_a^{SerO^- \bullet PO_4^{3-}}$ is set to values lower

than 100 nM. Thus, the PO_4^{3-} disassociation constant for deprotonated Ser102 AP must be greater than 100 nM.

$$K_a^{P_i^{observed}} = \left(\frac{1}{1+10^{pH-pK_a^{basic}}}\right)\times \left(\frac{K_a^{SerO^-\bullet(H)PO_4^{3-}}}{\left(1+10^{pK_a^{H_3PO_4}+pK_a^{H_2PO_4^{1-}}-2pH}+10^{pK_a^{H_2PO_4^{1-}}-pH}+10^{pH-pK_a^{HPO_4^{2-}}}\right)}+\frac{K_a^{SerO^-\bullet PO_4^{3-}}}{\left(1+10^{pK_a^{HPO_4^{2-}}+pK_a^{H_2PO_4^{1-}}+pK_a^{H_3PO_4}-3pH}+10^{pK_a^{HPO_4^{2-}}+pK_a^{H_2PO_4^{1-}}-2pH}+10^{pK_a^{HPO_4^{2-}}-pH}\right)}\right) \quad \text{(S15)}$$

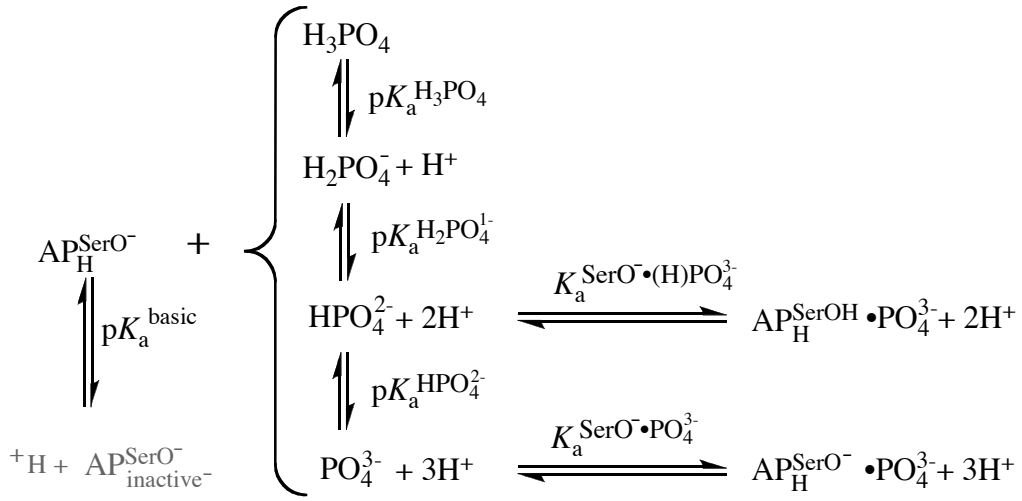

Scheme S3

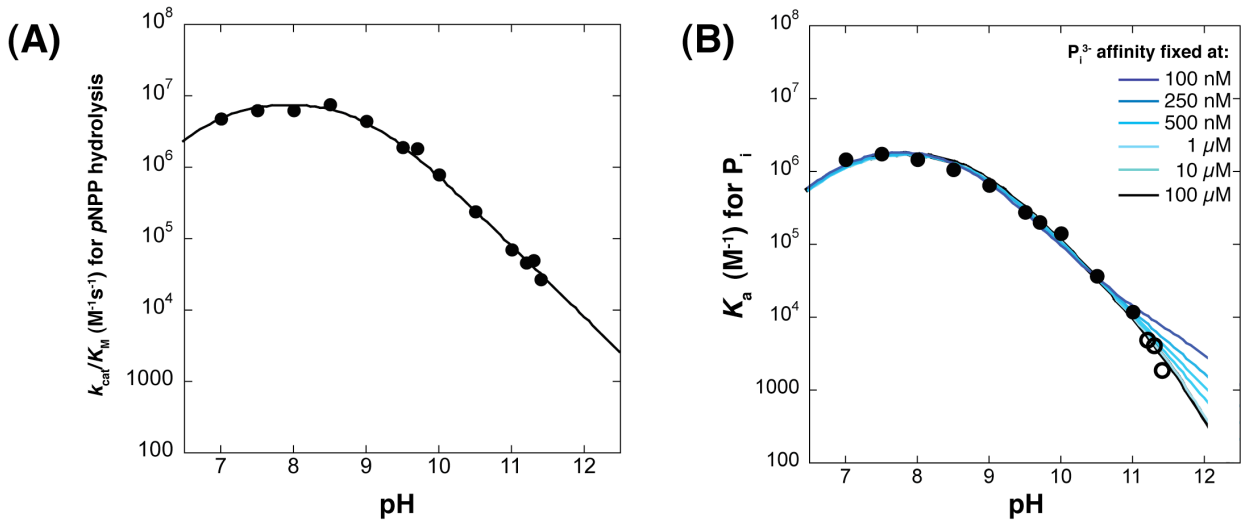

Figure S5. Analysis for PO_4^{3-} binding affinity for deprotonated Ser102 AP. The size of the data points corresponds to the estimated error of 20% (A) The pH-dependent *p*NPP hydrolysis activity of AP behaves predictably out to pH 11.4. Standard reaction assay conditions of 100 mM NaAcetate (pH 4.5-5.5), NaMaleic Acid (pH 6.0-6.5), NaMOPS (pH 7-8.0), NaCHES (pH 8.5-9.5), NaCAPS (pH 10-11.2), NaCABS (pH 11.0-11.4), 100 mM NaCl, 1 mM $MgCl_2$, and 100 μM $ZnCl_2$ were used at 25 °C. A non-linear least squares fit (Kaleidagraph, Synergy Software) of eq S14 yielded a fit with pK_a^{acidic} = 6.9, pK_a^{basic} = 8.9 and a $(k_{cat}/K_M)^{max}$ = 8.6 × 10^6 $M^{-1}s^{-1}$ in reasonable agreement with previous results.[17] (B) The pH-dependent P_i affinity of AP observed to pH 11.4 under the standard assay conditions above. The data from pH 7.0-11.0 (solid circles) were fit using a non-linear least squares fit of eq S15 at various fixed values of $K_a^{SerO^-\bullet PO_4^{3-}}$ corresponding to the $K_d^{SerO^-\bullet PO_4^{3-}}$ values shown. All fits gave $K_d^{SerO^-\bullet (H)PO_4^{3-}}$ values of ~0.5 μM and pK_a^{basic} ~ 8.7. The fit using a fixed $K_d^{SerO^-\bullet PO_4^{3-}}$ of 100 nM deviated 4-fold from the data from pH 11.0-11.4 (open circles) - a larger deviation than expected from the estimated error of these measurements (<50%).

Description of ground state destabilization via restriction in conformational freedom

As noted in the main text, interactions that increase the energy of the E•S state relative to the E+S and transition states are defined as ground state destabilizing (Figure 5C main text)[18-20], and the most common origin of ground state destabilization is likely a conformational entropy penalty arising from the binding and positioning of substrates in a restricted set of conformations such that the substrates are next to each other and next to reactive groups in the active site. This effect is easiest to appreciate for a bi-molecular reaction in which two substrates, S_1 and S_2, must come together to react (as depicted in Figure S6 for corresponding enzymatic and nonenzymatic

reactions). In both the nonenzymatic reaction and the enzymatic reaction starting from the free substrates and free enzyme there is a penalty in conformational entropy for positioning the reactants together in the transition state, formally resulting in the loss of several degrees of translational and rotational degrees of freedom for each reactant.[1]

We extend an analogy used by Jencks in terms of 'paying' the energetic price for a reaction.[18] Our enzyme is akin to a special VIP card that can be purchased upon entry to an amusement park that allows you to skip the long lines.[24] With this card, a barrier for entering a ride is removed since we pay less in waiting time for each ride once in the amusement park; with the enzyme we 'pay' less in energy to reach the transition state because a reaction barrier of conformational entropy has been removed or lessened. In other words, by forming the $E{\bullet}S_1{\bullet}S_2$ ground state, the loss in conformational entropy that must occur to accomplish the reaction is already paid for – it is paid for by the binding interactions that position the two substrates with respect to one another; in contrast, in the nonenzymatic reaction this entropic penalty must still be paid in the progression from the S_1+S_2 free state to the $S_1{\bullet}S_2^{\ddagger}$ transition state ($\Delta S^{\ddagger}_{solution}$ in Figure S6). Thus, the entropic component of the barrier for the nonenzymatic reaction is larger.[2] The enzyme-bound ground state is destabilized relative to a hypothetical enzyme that makes the same interactions with the substrates but accomplishes less restriction of motion of the substrates with

[1] Unfortunately, what we consider conceptually as 'entropy' is typically the freedom of motion of reactants, whereas experimental measures of ΔS includes all of the species present and, in practice, are often dominated by contributions from the surroundings –solvent molecules and/or the enzyme. Deconvolution of these contributions is an unmet challenge, although there is interesting work in this area.[21-23]

[2] In the amusement park, with your VIP card you are positioned at the start of the ride, whereas those who cannot afford the card have to start at the back of the line and experience a longer path – or larger conformational barrier – to get to the ride.

respect to one another.[3] Thus, the enzyme selectively destabilizes the ground state, as depicted in Figure 5C in the main text. The same arguments can be made for single substrate reactions for which binding positions the substrate with respect to catalytic groups on the enzyme, analogous to positioning substrates with respect to one another as described above.

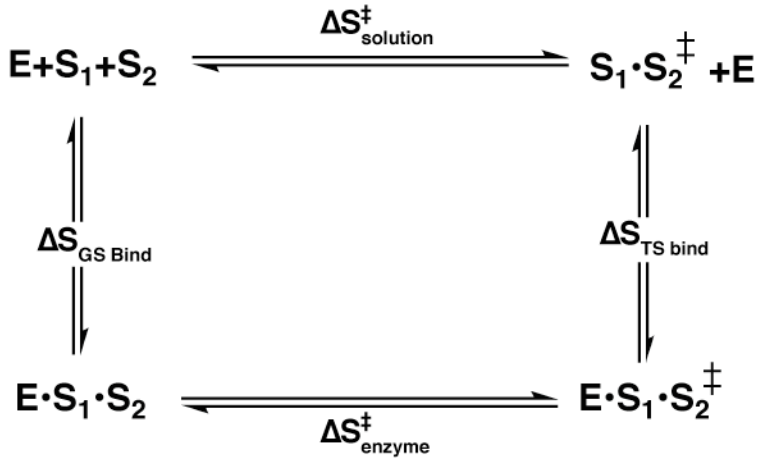

Figure S6. Thermodynamic cycle illustrating considerations of conformational entropy for enzyme-catalyzed and solution reactions. As noted in the main text, we use the terms entropy and conformational entropy here to refer to the degree of restriction in freedom of motion of the substrates with respect to one another, although these properties cannot yet be parsed experimentally. The entropic penalty for the solution reaction ($\Delta S^{\ddagger}_{solution}$) is larger than the entropic penalty for the enzymatic reaction ($\Delta S^{\ddagger}_{enzyme}$) because binding energy is used to offset the conformational entropy cost ($\Delta S^{\ddagger}_{enzyme} < \Delta S^{\ddagger}_{solution}$). Utilization of binding energy to align substrates for reaction results in an apparent destabilization of the enzyme ground state relative to a hypothetical enzyme that provides less conformational restriction of its substrates but maintains the same binding interactions and thus achieves stronger binding. For an ideal case in which the enzyme precisely positions the reactants, there would be little or no additional conformational restrictions upon forming $E \bullet S_1 \bullet S_2^{\ddagger}$ from $E \bullet S_1 \bullet S_2$ ($\Delta S^{\ddagger}_{enzyme}$ negligible). Independent motion is restricted in the $S_1 \bullet S_2^{\ddagger}$ nonenzymatic transition state by definition, due to formation of a partial covalent bond between the substrates. Thus, less confromational entropy is lost upon association of the transition state with the enzyme than upon association of the two substrates with the enzyme ($\Delta S_{TS\ Bind} < \Delta S_{GS\ Bind}$).

[3] Many of the comparisons made in describing energetic concepts are crude approximations of physical behavior but are nevertheless useful as idealized examples that allow us to better understand the underlying energetic concepts. Indeed, we are still unable to fully describe the conformational states and energetics of enzymatic reactions; this remains a major challenge.

Supporting References

(1) Lad, C.; Williams, N. H.; Wolfenden, R. *Proc. Natl. Acad. Sci. U.S.A.* **2003**, *100*, 5607-5610.
(2) Lassila, J. K.; Zalatan, J. G.; Herschlag, D. *Annu. Rev. Biochem.* **2011**, *80*, 669-702.
(3) Martell, A. E.; Smith, R. M. *Critical Stability Constants, Vol. 1-6* **1989**, *Plenum Press, New York*.
(4) O'Brien, P. J.; Herschlag, D. *Biochemistry* **2002**, *41*, 3207-3225.
(5) Jencks, W. P.; Regenstein, J. In *Handbook of Biochemistry and Molecular Biology*; Fasman, G. D., Ed.; CRC: Cleveland, OH, 1976.
(6) Bounaga, S.; Laws, A. P.; Galleni, M.; Page, M. I. *Biochem J.* **1998**, *331*, 703-711.
(7) Mock, W. L.; Tsay, J. T. *J. Biol. Chem.* **1988**, *263*, 8635-8641.
(8) Pocker, Y.; Bjorkquist, D. W. *Biochemistry* **1977**, *16*, 5698-5707.
(9) Chlebowski, J.; Armitage, I.; Tusa, P.; Coleman, J. *J. Biol. Chem.* **1976**, *251*, 1207-1261.
(10) Gettins, P.; Coleman, J. E. *J. Biol. Chem.* **1983**, *258*, 408-416.
(11) Chlebowski, J. F.; Armitage, I. M.; Coleman, J. E. *J. Biol. Chem.* **1977**, *252*, 7053-7061.
(12) Schwartz, J. H. *Proc. Natl. Acad. Sci. U.S.A.* **1963**, *49*, 871-878.
(13) Cheng, H.; Nikolic-Hughes, I.; Wang, J. H.; Deng, H.; O'Brien, P. J.; Wu, L.; Zhang, Z.-Y.; Herschlag, D.; Callender, R. *J. Am. Chem. Soc.* **2002**, *124*, 11295-11306.
(14) Wang, J. H.; Xiao, D. G.; Deng, H.; Webb, M. R.; Callender, R. *Biochemistry* **1998**, *37*, 11106-11116.
(15) Cheng, H.; Sukal, S.; Deng, H.; Leyh, T.; Callender, R. *Biochemistry* **2001**, *40*, 4035-4043.
(16) Deng, H.; Lewandowicz, A.; Schramm, V. L.; Callender, R. *J. Am. Chem. Soc.* **2004**, *126*, 9516-9517.
(17) O'Brien, P. J.; Herschlag, D. *J. Am. Chem. Soc.* **1998**.
(18) Jencks, W. P. *Advances in Enzymology* **1975**, *43*, 219-410.
(19) Jencks, W. P. *Cold Spring Harb. Symp. Quant. Biol.* **1987**, *52*, 65-73.
(20) Murphy, D. *Biochemistry* **1995**, *34*, 4507-4510.
(21) Kraut, D. A.; Carroll, K. S.; Herschlag, D. *Annu. Rev. Biochem.* **2003**, *72*, 517-571.
(22) Frederick, K. K.; Marlow, M. S.; Valentine, K. G.; Wand, A. J. *Nature* **2007**, *448*, 325-329.
(23) Marlow, M. S.; Dogan, J.; Frederick, K. K.; Valentine, K. G.; Wand, A. J. *Nat. Chem. Biol.* **2010**, *6*, 352-358.
(24) Mohney, C. *Slate Online Magazine* **2002**, *http://www.slate.com/id/2067672/*.